

# The effect of elastic disorder on single electron transport through a buckled nanotube

S.S. Evseev,<sup>1,2</sup> I.S. Burmistrov,<sup>2</sup> K.S. Tikhonov,<sup>3,2</sup> and V. Yu. Kachorovskii<sup>4,5</sup>

<sup>1</sup>Moscow Institute for Physics and Technology, 141700 Moscow, Russia

<sup>2</sup>L. D. Landau Institute for Theoretical Physics, acad. Semenova av. 1-a, 142432 Chernogolovka, Russia

<sup>3</sup>Skolkovo Institute of Science and Technology, 143026 Moscow, Russia

<sup>4</sup>Ioffe Institute, Polytechnicheskaya 26, 194021, St.Petersburg, Russia St. Petersburg, Russia

<sup>5</sup>CENTERA Laboratories, Institute of High Pressure Physics, Polish Academy of Sciences, 01-142, Warsaw, Poland

We study transport properties of a single electron transistor based on elastic nanotube in the Coulomb blockade regime. We assume that the external compressive force is applied to the nanotube and focus on the vicinity of the Euler buckling instability. We demonstrate that in this regime the current–voltage characteristics of the transistor is extremely sensitive to random elastic disorder. In particular, the threshold value of a bias voltage beyond which the transport current flows is parametrically enhanced by random curvature and an additional plateau in dependence of the average current on a bias voltage appears.

A global trend of modern electronics is the design of nanodevices with ultra-low power consumption and a high level of integration. One of the most attractive candidates for this purpose is a single-electron transistor (SET) which is a sensitive electronic device based on the Coulomb blockade effect. Key points of fundamental physics of SET and its operation as a tunable nanodevice have been formulated about 20 years ago (for review see [1–5]). There has recently been an increased interest to this topic partially associated with the discovery of carbon systems with a transverse degree of freedom, such as suspended nanotubes and graphene. The interest is motivated by creation of nanoelectromechanical systems (NEMS) which are a class of devices integrating electrical and mechanical functionality on the nanoscale [6–16]. The simplest model of SET-based NEMS is provided by a harmonic mechanical oscillator coupled to an excess particle number on the SET island [14–23].

When suspended elastic nanotube is used as a SET island, coupling between mechanical and charge degrees of freedom provides an additional control via mechanical forces. This coupling can be strongly increased by applying a compressive force driving the nanotube towards the Euler buckling instability [24, 25] (see more recent experimental [27–34] and theoretical [14–16, 35–38, 40–42] studies of this instability). Physics of such systems is captured by the model developed in Ref. [14–16]. This model was focused on the study of a SET made of a clean nanotube in which fluctuations arise only due to a finite temperature. In fact, the extreme sensitivity of the nanomechanical SET to an external environment implies that presence of disorder can strongly modify the obtained results. The effect of disorder is twofold. First of all, disorder can change the effective potential well confining electron in the island. This effect is small and can be fully taken into account by small correction to the capacitance. The much stronger effect is expected due to an elastic disorder. As was shown in Refs. [39–42], such disorder can strongly affect buckling transition especially

near the instability.

In this Letter we develop the theory of disordered nanomechanical SET (see Fig. 1). We model disorder by spontaneous local curvature [39–42]. We will demonstrate that the results obtained in Refs. [14–16] for a *clean* nanomechanical SET are strongly modified in the presence of disorder. In particular, the threshold value of a bias voltage needed for the current to flow through the SET can be dramatically enhanced (see Fig. 2). Also we predict a disorder-induced plateau in the dependence of the average current on bias voltage.

**MODEL.** The sketch of the setup is shown in Fig. 1 (left panel). We consider a nanotube suspended between left (L) and right (R) leads (serving as source and drain, respectively). The tunneling coupling of the nanotube to the source (drain) is characterized by the tunneling rates  $\Gamma_L$  ( $\Gamma_R$ ). We assume that a finite voltage bias  $V$  is applied between source and drain shifting their chemical potentials to  $\pm eV/2$ . The electrical potential  $V_g$  of the nanotube can be tuned by a capacitively coupled electrode (gate). We consider the limit of a relatively short nanotube and very strong Coulomb blockade such that there is a single energy level on the nanotube that can be singly occupied by an electron from leads. General-

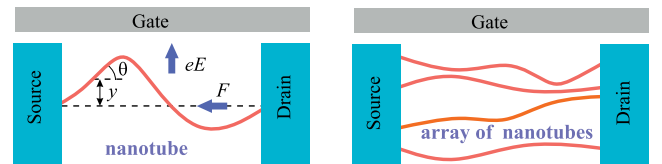


FIG. 1. Sketch of a possible realization of SETs with an elastic degree of freedom. Left: A SET with a suspended nanotube driven by external force  $F$  close to the buckling transition forms a SET tunnel-coupled to a source and a drain. A gate electrode creates additional electric field  $E$  in the  $y$  direction. Provided the nanotube is occupied by an electron, the transverse electric field  $E$  bends the nanotube. Right: A SET made of an array of nanotubes.

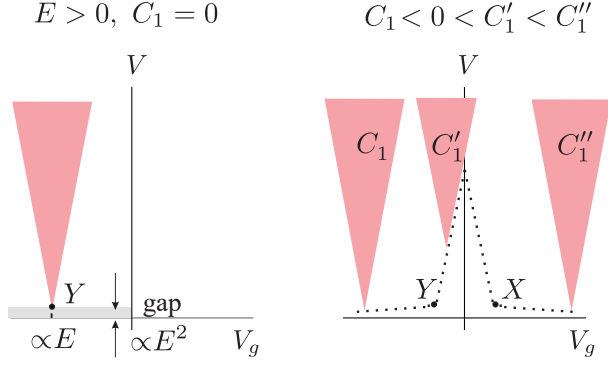


FIG. 2. Schematic plot of the current density in  $(V_g, V)$  plane for different values of  $E$  and for a different realizations of a random curvature, characterized by disorder strength,  $C_1$ . Regions with non-zero current are marked by pink color (see text).

ization on transport through higher levels of size quantization is straightforward (see Ref.[15] for discussion of clean case). The Hamiltonian describing the elastic degrees of freedom (parametrized by the bending angle  $\theta$  as a function of the arc-length position  $s$ , see Fig. 1) and their coupling to electrons reads

$$\hat{H} = \int_0^L ds \left[ \kappa(\theta' - C')^2/2 + F \cos \theta \right] + eE \hat{n}_d Y, \quad (1)$$

where  $\theta' \equiv d\theta/ds$  and  $Y = \int_0^L |\psi_0(s)|^2 y(s) ds$  is the average displacement of the nanotube in  $y$  direction. Here  $\kappa$  denotes the bending rigidity of the nanotube,  $F$  stands for the compressing force applied to the ends of the nanotube, and  $E$  is an additional electric field created by the gate electrode, directed along  $y$  axis. The electronic degrees of freedom enters the Hamiltonian (1) via the operator of the excess particle number,  $\hat{n}_d$ , and the wave function,  $\psi_0(s)$ , of an active electron energy level on the nanotube. Provided the nanotube is occupied by an electron, the transverse electric field  $E$  bends the nanotube. The nanotube is assumed to be clamped on the left and right reservoirs of the SET, such that Hamiltonian (1) has to be supplemented by the following curvature-dependent boundary conditions [39, 40],

$$y(0) = y(L), \quad \theta'(0) = C'(0), \quad \theta'(L) = C'(L). \quad (2)$$

In the Hamiltonian (1) we neglect the elastic kinetic energy. This is justified under assumption that a typical elastic frequency of transverse oscillations of the nanotube,  $\omega \propto \sqrt{\kappa/(\rho L^4)}$ , where  $\rho$  is the linear mass density of the nanotube, is small as compared to temperature,  $\hbar\omega \ll T$ . As a result, the only dynamical degree of freedom in the Hamiltonian (1) is the excess particle number,  $\hat{n}_d$ . In the strong Coulomb blockade regime, the operator  $\hat{n}_d$  takes two values,  $n_d=0$  and  $n_d=1$ . Solution of the coupled — electronic and elastic — dynamical problem

can be essentially simplified in the adiabatic approximation provided the tunneling between the nanotube and the source and the drain is sufficiently fast,  $\Gamma_{L,R} \gg \omega$ . In such adiabatic approximation and under assumption,

$$\hbar\Gamma_{R,L} \ll \max\{T, |eV|, |eV_g|\}. \quad (3)$$

one can replace the operator  $\hat{n}_d$  with its average value for a fixed configuration  $y(s)$  (or, equivalently,  $\theta(s)$ ) [15]

$$n_d(Y) = \sum_{\lambda=\pm} \gamma_\lambda f_F(eEY - eV_\lambda), \quad (4)$$

Here  $f_F(\varepsilon) = 1/[\exp(\varepsilon/T) + 1]$  denotes the Fermi function,  $V_\lambda = V_g + \lambda eV/2$ ,  $\gamma_- = \Gamma_L/(\Gamma_L + \Gamma_R)$ , and  $\gamma_+ = 1 - \gamma_-$ . Under conditions (3), the current through the SET reads

$$\mathcal{I}(Y) = 2e\Gamma I(Y), \quad I(Y) = \sum_{\lambda=\pm} \frac{\lambda}{2} f_F(-eEY + eV_\lambda), \quad (5)$$

where  $\Gamma = \Gamma_L \Gamma_R / (\Gamma_L + \Gamma_R)$ .

In the adiabatic approximation the problem for the computation of the bending angle becomes fully classical and the bending angle profile is described by the following nonlinear equation,

$$\kappa(\theta''(s) - C''(s)) + F \sin \theta(s) = eE(s)n_d(Y) \cos \theta(s), \quad (6)$$

where  $E(s) = E \int_s^L ds' |\psi_0(s')|^2$ . Hereafter we assume  $T=0$  and shall estimate the effect of thermal fluctuations at the end of the paper. The energy corresponding to Eq. (6) is obtained from the Hamiltonian (1) by substitution of  $\int_0^Y d\mathcal{Y} n_d(\mathcal{Y})$  for  $\hat{n}_d Y$ , where  $n_d(Y) = \sum_{\lambda=\pm} \gamma_\lambda \Theta(V_\lambda - eEY)$ . Here  $\Theta(x)$  denotes the Heaviside step function.

**FUNDAMENTAL MODE APPROXIMATION.** In order to satisfy the boundary conditions (2), it is convenient to expand the functions  $\theta(s)$  and  $C(s)$  in the Fourier series,

$$\theta(s) = \sum_{n=1}^{\infty} \theta_n \cos q_n s, \quad C(s) = \sum_{n=1}^{\infty} C_n \cos q_n s, \quad (7)$$

where  $q_n = \pi n/L$ . Euler buckling instability is clearly seen from Eq. (6) at  $E=0$ . Indeed, linearization of this equation yields divergence of  $\theta_1$  for  $F = F_c = \kappa(\pi/L)^2$ :  $\theta_1 \approx -8C_1/\epsilon$ , where  $\epsilon = 8(F - F_c)/F_c$ . Hereafter we assume that  $|\epsilon| \ll 1$ . In fact, the growth of  $\theta_1$  for  $|\epsilon| \rightarrow 0$  is limited by nonlinear terms in the Eq. (6). The modes  $\theta_n$  with  $n \geq 2$  are finite at  $F = F_c$  and can be computed within the linear approximation. Such crucial difference between the behavior of the mode with  $n=1$  and modes with  $n \geq 2$  allows us to project Eq. (6) onto the fundamental mode  $\cos(q_1 s)$  as it was done in the clean case [14, 15]. Then, under assumption  $|\theta_1| \ll 1$ , the nonlinear equation (6) is reduced to

$$\theta_1^3 - \epsilon \theta_1 + \alpha n_d(\theta_1) = 8C_1, \quad n_d(\theta_1) = \sum_{\lambda=\pm} \gamma_\lambda \Theta(v_\lambda - \theta_1). \quad (8)$$

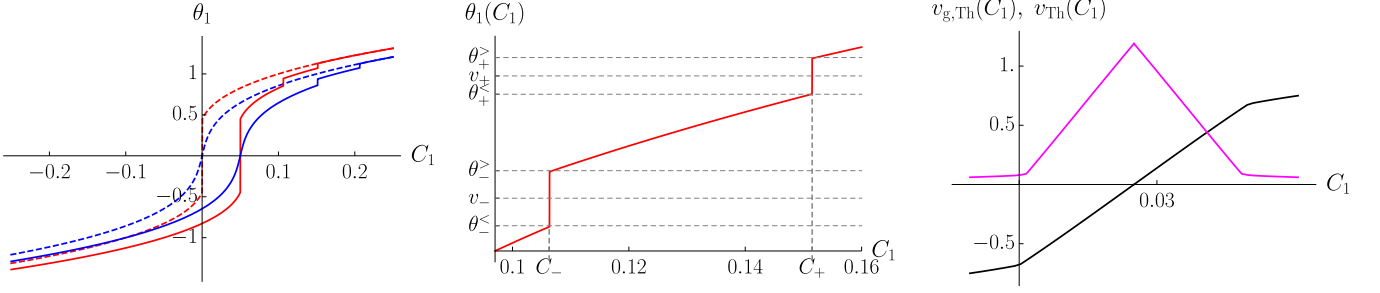


FIG. 3. Left: Example of the dependence of  $\theta_1$  corresponding to the absolute minimum of the energy  $W$  on the disorder strength  $C_1$  for  $\epsilon = \pm 0.2$  at  $\alpha = 0$  (dashed red and blue curves) and at  $\alpha = 0.4$  (red and blue curves). Middle: Zoom of  $\theta_1(C_1)$  dependence from the left panel (for  $\epsilon = 0.2$ ) in the vicinity of the jumps. Right: Dependence of  $v_{\text{Th}}$  and  $v_{g,\text{Th}}$  on  $C_1$  (magenta and black curves, respectively) for  $\epsilon = 0.2$  and  $\alpha = 0.4$ . For all panels  $v_g = 1$ ,  $v = 0.2$ , and  $\gamma_{\pm} = 1/2$ .

Here we introduced  $v_{\pm} = v_g \pm v/2$  where the dimensionless voltages  $v_g = \pi V_g / (a_1 E L)$  and  $v = \pi V / (a_1 E L)$  as well as the dimensionless strength of the electron-phonon interaction [43]

$$\alpha = \frac{16a_1 e E}{\pi F_c}, \quad a_n = \int_0^L ds |\psi_0(s)|^2 \sin(q_n s). \quad (9)$$

We note that for  $\psi_0(s) = \sqrt{2/L} \sin(q_1 s)$  one finds the constant  $a_1 = 8/(3\pi)$ . At low enough  $T$  we are interested in the solution  $\theta_1(C_1)$  of Eq. (8) that provides the minimum of the energy  $\tilde{H} \mapsto \pi^2 \kappa W(\theta_1)/(16L)$ , where

$$W(\theta_1) = \theta_1^4/4 - \epsilon \theta_1^2/2 + \alpha w_d(\theta_1) - 8C_1 \theta_1, \quad (10)$$

with  $w_d(\theta_1) = \sum_{\lambda=\pm} \gamma_{\lambda} [(\theta_1 - v_{\lambda})\Theta(v_{\lambda} - \theta_1) + v_{\lambda}\Theta(v_{\lambda})]$ . For  $\alpha = 0$  the energy  $W(\theta_1)$  has the form of the Landau expansion of the free energy in series of the order parameter ( $\theta_1$ ) near the second order phase transition at  $\epsilon = 0$ . The random curvature  $C_1$  plays the role of the magnetic field that breaks the symmetry between two states of minimal energy at  $\epsilon > 0$ . Hence, the system can show the hysteretic behavior. However, since we focus here in dc current, we assume that the system always has time to reach the absolute energy minimum. The term  $\alpha w_d(\theta_1)$  suppresses the bistability thus competing with the random curvature. Most importantly, single-mode approximation allows one to find the  $I - V$  curve for a fixed disorder realization and also to calculate analytically the disorder averaged current.

**CURRENT.** For a given value of  $C_1$  there is the unique solution  $\theta(C_1)$  of Eq. (8) that implements the absolute minimum of  $W$ . Due to the presence of  $v_{\pm}$  in the expression for  $n_d(\theta_1)$ , the solution  $\theta(C_1)$  depends on gate and bias voltages. The example of such a solution is shown in the Fig. 3. As seen from the Fig. 3, there are two major effects of the electro-mechanical coupling ( $\alpha \neq 0$ ): (i) the curve  $\theta_1(C_1)$  becomes asymmetric with respect to the inversion:  $\theta_1 \mapsto -\theta_1$  and  $C_1 \mapsto -C_1$ ; (ii) one or two

vertical mini-jumps can form on this dependence in addition to the large jump at  $C_1 = 0$ . On the right panel of Fig. 3, we zoom the region corresponding to these mini-jumps (they occur at particular values of curvature  $C_{\pm}$ ). Let us denote the boundary values of  $\theta_1$  at these mini-jumps as  $\theta_{-}^{\leq} < v_{-} < \theta_{+}^{\leq}$  and  $\theta_{+}^{\leq} < v_{+} < \theta_{+}^{\geq}$  (see Fig. 3). The parameters  $\theta_{\pm}^{>/<}$  satisfy the following equations,

$$C_{\lambda} \equiv C_1(\theta_{\lambda}^{\geq}) = C_1(\theta_{\lambda}^{\leq}), \quad W(\theta_{\lambda}^{\geq}) = W(\theta_{\lambda}^{\leq}). \quad (11)$$

In accordance with Eqs. (11) not only the width of the jump  $\theta_{+}^{\geq} - \theta_{+}^{\leq}$  but also its position,  $C_{\lambda}$ , depends on  $v_{\lambda}$ . For a given value  $C_1$  the current is given as (we assume that  $v \geq 0$ ),

$$I = \sum_{\lambda=\pm} \frac{\lambda}{2} \Theta(v_{\lambda} - \theta_1(C_1)) = \begin{cases} 1/2, & \theta_{-}^{\geq} < \theta_1(C_1) < \theta_{+}^{\leq}, \\ 0, & \text{otherwise.} \end{cases} \quad (12)$$

As follows from Eq. (12), the current is equal 1/2 for such values of  $v_g$  and  $v$  that satisfy  $C_{-} < C_1 < C_{+}$ . As one can check, the function  $C_{\pm}(v_{\pm})$  is a monotonous function of its argument. As a result, the current equals 1/2 in a diamond region,  $v > \max\{2v_g - 2v_{-}(C_1), -2v_g + 2v_{+}(C_1)\}$ , in the  $v$  versus  $v_g$  plane (see Fig. 2, right panel). Here  $v_{\pm}(C_1)$  are solutions of the equations  $C_{\pm}(v_{\pm}) = C_1$ . For a given  $C_1$  there is the minimal threshold for a bias voltage  $v_{\text{Th}}$  at which current begins to flow. This minimal threshold bias voltage realizes at the certain gate voltage  $v_{g,\text{Th}}$ . These threshold voltages can be found as follows

$$v_{\text{Th}} = v_{+}(C_1) - v_{-}(C_1), \quad v_{g,\text{Th}} = (v_{+}(C_1) + v_{-}(C_1))/2. \quad (13)$$

Equation (13) determines the function  $v_{\text{Th}}(v_g)$  in the parametric form. Independently of the magnitude of  $C_1$ , the current is zero for  $v < v_{\text{Th}}(v_g)$ . With decrease of  $C_1$  from positive values to negative values the diamond of nonzero current is moving along the curve  $v_{\text{Th}}(v_g)$  as shown in Fig. 2 (right panel).

In the case of the symmetric junction,  $\gamma_{\pm} = 1/2$ , there is a relation  $v_{-}(C_1) = v_{+}(C_1 - \alpha/16)$  and the

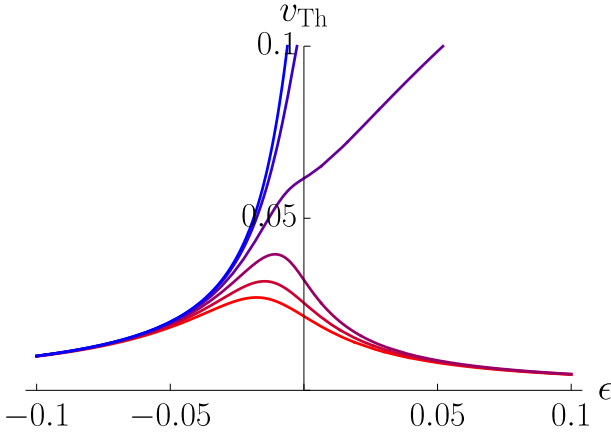


FIG. 4. Dependence of the threshold voltage,  $v_{\text{Th}}$ , on  $\epsilon$  at different values of  $C_1$  ranging from  $-1.25 \cdot 10^{-4}$  to  $1.25 \cdot 10^{-4}$  (from red to blue) with the step  $0.5 \cdot 10^{-4}$ . The parameter  $\alpha = 2 \cdot 10^{-3}$  and  $\gamma_{\pm} = 1/2$ .

function  $v_+(C_1)$  is antisymmetric with respect to the point  $\alpha/32$ ,  $v_+(-C_1 + \alpha/32) = -v_+(C_1 - \alpha/32)$ . Consequently, one finds  $v_{g,\text{Th}} = 0$  at  $C_1 = \alpha/16$  as well as  $v_{g,\text{Th}}(0) = -v_{g,\text{Th}}(\alpha/8)$  and  $v_{\text{Th}}(0) = v_{\text{Th}}(\alpha/8)$ . Thus the curve  $v_{\text{Th}}(v_g)$  is symmetric with respect to  $v_g \mapsto -v_g$  and has the maximum at  $v_g = 0$ .

The dependence of the threshold voltage,  $v_{\text{Th}}$ , on the dimensionless buckling force  $\epsilon$  is shown in Fig. 4. As one can see, this dependence is very sensitive to disorder. The change of  $C_1$  from  $-\alpha/16$  to  $\alpha/16$  results in qualitative change of the behavior of  $v_{\text{Th}}$  with  $\epsilon$ . For  $\epsilon > 0$  the disorder enhances parametrically the threshold voltage.

**DISTRIBUTION FUNCTIONS.** The distribution function of the bending angle can be expressed in terms of the probability distribution function (PDF) of a random curvature,  $P(C_1)$ , and the function  $C_1 = C_1(\theta_1)$  which is the inverse function for the function  $\theta_1(C_1)$ ,

$$\mathcal{P}(\theta_1) = \left[ \frac{d\theta_1(C_1)}{dC_1} \right]^{-1} P(C_1) \Big|_{C_1=C_1(\theta_1)}. \quad (14)$$

The jumps of  $\theta_1$  in the dependence  $\theta_1(C_1)$  result in appearance of regions at which  $\mathcal{P}(\theta_1)$  is identically zero. In particular,  $\mathcal{P}(\theta_1) \equiv 0$  for  $\theta_{\pm}^< < \theta_1 < \theta_{\pm}^>$ . A typical example of  $\mathcal{P}(\theta_1)$  is shown in the left panel of Fig. 5 under assumption that  $C_1$  has the normal distribution,  $P(C_1) = \exp[-C_1^2/(2\Delta_1)]/\sqrt{2\pi\Delta_1}$ .

At low temperatures the PDF for the current becomes

$$\mathcal{P}(I) = \langle I \rangle \delta(I - 1/2) + (1 - \langle I \rangle) \delta(I). \quad (15)$$

Here the average current contains information about the PDF of the random curvature,

$$\langle I \rangle = \frac{1}{2} \int_{\theta_{-}^>}^{\theta_{+}^<} d\theta_1 \mathcal{P}(\theta_1) = \frac{1}{2} \Theta(C_+ - C_-) \int_{C_-}^{C_+} dC_1 P(C_1). \quad (16)$$

The above expression suggests that the average current cannot exceed the value  $1/2$ . The average current as the function of  $v$  and  $v_g$  is shown in the middle panel of Fig. 5. At fixed  $v_g$ , the value  $1/2$  for the current is reached at large values of  $v$  when both  $C_{\pm} \rightarrow \pm\infty$ . For  $v_g > 0$  there is a broad interval of  $v$  at which the current is neither zero nor  $1/2$ . Such intermediate step in the current-voltage dependence occurs then  $C_+$  has large positive value (in comparison with  $\sqrt{\Delta_1}$ ) whereas  $C_-$  is pinned to the value of the order of  $\alpha$ . Therefore, the existence of this feature in the current reflects the competition between two symmetry breaking mechanisms: electron-phonon coupling and elastic disorder. For  $\alpha \ll \sqrt{\Delta_1}$  the intermediate step is present whereas for  $\alpha \gg \sqrt{\Delta_1}$  is suppressed (see Fig. 5, right panel).

**DISCUSSION.** The higher harmonics of  $\theta_n$  ( $n \geq 2$ ) can be obtained from Eq. (6) by expansion to the linear order in  $\theta(s)$ ,  $\theta_n \simeq n^2 [C_n - \alpha a_n n_d(\theta_1)/(8n^3 a_1)]/(n^2 - 1)$ . Taking them in account, we find that Eq. (8) remains valid but shift of the critical force occurs,  $\epsilon \mapsto \epsilon + \delta\epsilon$ , where  $\delta\epsilon = -2 \sum_{n=2}^{\infty} \theta_n(\theta_n + \theta_{n+2})$ . As we demonstrated above the most interesting regime for a given curvature is  $|C_1| \sim \alpha$ . Assuming that in this regime the higher harmonics of disorder  $C_n$  are of the same order, we find that the shift of the critical buckling force is irrelevant at  $\alpha \ll |\epsilon|$ . For the case of a random curvature distribution one needs to additionally average the r.h.s of Eq. (14) over the distribution of  $\delta\epsilon$  and, then, use the modified  $\mathcal{P}(\theta_1)$  in Eq. (16).

Now we discuss the effect of nonzero temperature. For a clean SET these effects were analyzed in Refs. [14–16]. The current depends on  $T$  due to at least two reasons. At first, there are thermal fluctuations of the generalized coordinate  $Y$ . In the fundamental mode approximation these fluctuations of the bending angle are described by the Gibbs factor  $\exp(-W_{\text{eff}}(\theta_1)/T)$  where  $W_{\text{eff}}(\theta_1)$  is given by Eq. (10) with  $w_d(\theta_1) = \sum_{\lambda=\pm} \tilde{T} \gamma_{\lambda} \ln[f_F(\alpha(v_{\lambda} - \theta_1))/f_F(\alpha v_{\lambda})]$  (see Eqs. (19), (25) of Ref. [16]). The effective dimensionless temperature is defined as

$$\tilde{T} = 16LT/(\pi^2 \kappa). \quad (17)$$

With neglect of electron-phonon coupling, i.e. at  $\alpha = 0$ , the thermal fluctuations are characterized by  $\delta\theta_1^{(T)} \sim (\tilde{T}/\epsilon)^{1/2}$ . Secondly, temperature enters the Fermi distribution function in the expression (5) for the current. Therefore, for a given curvature the temperature results in broadening of a boundary of the Coulomb blockade diamond. For a random curvature distributed continuously, the average current is given as the average over  $P(C_1)$  and the Gibbs weight  $\exp(-W_{\text{eff}}(\theta_1)/\tilde{T})$ . The result of this computation is shown on the Fig. 5, right panel. It illustrates blurring of the disorder-induced step in the  $I(v)$  curve at intermediate voltages by a finite temperature. To estimate the temperature at which the disorder-induced step will be smeared out we compare

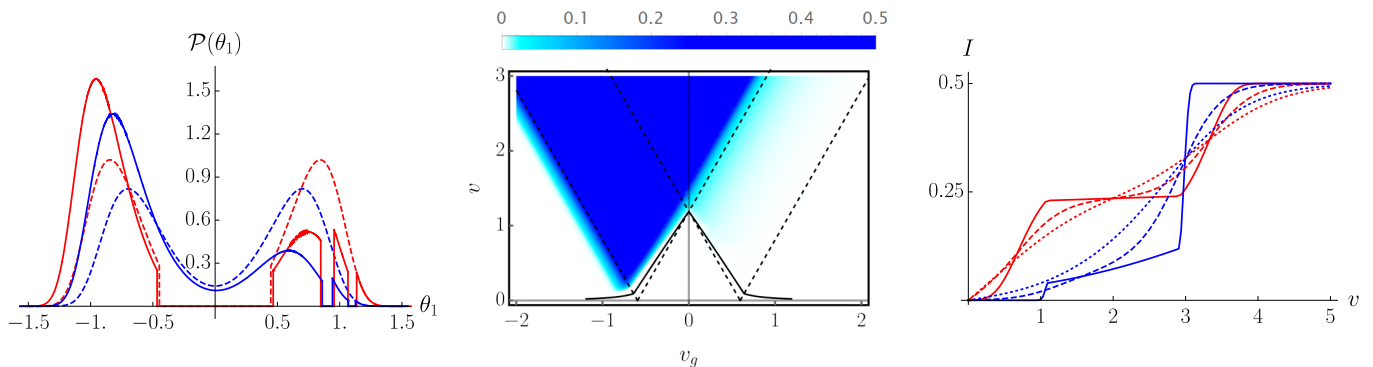


FIG. 5. The case of symmetric junction  $\gamma_{\pm}=1/2$ . Left: PDF as determined by Eq. (14) for  $\alpha=0$  and  $\alpha=0.4$ . The other parameters are  $\epsilon=\pm 0.2$  (red and blue curves, respectively),  $v_g=1$ ,  $v=0.2$ , and  $\Delta_1=5 \cdot 10^{-3}$ . Middle: Phase diagram and density plot of the current for  $\epsilon=0.2$ ,  $\alpha=0.4$ , and  $\Delta_1=2 \cdot 10^{-4}$ . The black solid curve is the threshold  $v_{\text{Th}}(v_g)$ . The dashed straight lines are given by following relations  $v=\pm v_{\text{Th}}(v_g=0)\pm 2v_g$ . Right: The current-voltage characteristics for  $v_g=1$  (red and blue traces, respectively),  $\alpha=0.02$  for different values of disorder  $\Delta_1=8 \cdot 10^{-4}$  and  $\Delta_1=3 \cdot 10^{-6}$  (red and blue correspondingly) for  $\tilde{T}=0, 0.125, 0.250$  (solid, dashed, dotted curves, respectively).

$\delta\theta_1^{(T)}$  with the width of the zero temperature PDF,  $\mathcal{P}(\theta_1)$ . For a normally distributed  $C_1$ , in the limit of weak disorder,  $\Delta_1 \ll \epsilon^2$ , the latter can be estimated  $\delta\theta_1^{(\text{dis})} \sim \sqrt{\Delta_1}/\epsilon$ . We thus find that the temperature blurring of the intermediate plateau is negligible at temperatures  $\tilde{T} \ll \Delta_1/\epsilon$ .

Recently, a possibility of a complete control of a SET by means of an external mechanical forces has been clearly demonstrated experimentally [31–34]. In very recent experimental work [33] a double-well elastic potential describing collective coordinate  $Y$  was created and controlled mechanically by using two mechanical forces corresponding to  $F$  and  $E$  in our model. In Ref. [31] the lowest-lying flexural eigenmodes of nanotube were identified with an unprecedented precision by capacitively driving the nanotube-based mechanical resonator with an external circuit. Excitation of such eigenmodes by placing the nanotube into the optical cavity shows surprisingly high quality factors (up to  $10^4$ !) [32]. The latter implies extreme sensitivity of suspended nanotubes to external forces. SET coupled to oscillating field was realized in Ref. [34] and field-driven Coulomb blockade peaks were used to make a single-electron “chopper”.

Based on Refs. [12, 13], the authors of Ref. [15] estimated the strength of electron-phonon coupling which corresponds to  $\alpha \sim 10^{-4} \div 10^{-3}$ . At the same time, using Ref. [44] we can roughly estimate  $C_1=0.1 \div 1$ . The above estimates imply that disorder dominates electron transport through a nanotube-based SET for typical values of experimental parameters. One of the most interesting problems to be solved in future is to study effect of disorder on high-quality resonances observed in Refs. [31–34].

To summarize, we considered transport properties of a single electron transistor based on elastic nanotube with a random curvature in the strong Coulomb blockade regime. We studied the vicinity of the Euler buckling instability and demonstrated that close to buckling transi-

tion, the current-voltage characteristics of the transistor is extremely sensitive to a random curvature. In particular, we predicted existence of an additional plateau in dependence of the average current on a bias voltage. Our predictions can be tested experimentally in systems similar to ones studied in Refs. [31–34].

**ACKNOWLEDGEMENT.** We thank I. Gornyi for useful comments and discussions. The work was funded in part by Russian Foundation for Basic Research (grant No. 20-52-12019) – Deutsche Forschungsgemeinschaft (grant No. SCHM 1031/12-1) cooperation. VK was partially supported by Foundation for the Advancement of Theoretical Physics and Mathematics (BASIS) and by IRAP Programme of the Foundation for Polish Science (grant MAB/2018/9, project CENTERA).

- 
- [1] *The special issue on single charge tunneling*, Z. Phys. B **85**, 317 (1991).
  - [2] M. A. Kastner, *The single-electron transistor*, Rev. Mod. Phys. **64**, 849 (1992).
  - [3] *Single Charge Tunneling*, ed. by H. Grabert and M. H. Devoret (Plenum, New York, 1992)
  - [4] W. G. van der Wiel, S. De Franceschi, J. M. Elzerman, T. Fujisawa, S. Tarucha, L. P. Kouwenhoven, *Electron transport through double quantum dots*, Rev. Mod. Phys. **75**, 1 (2002).
  - [5] R. Hanson, L. P. Kouwenhoven, J. R. Petta, S. Tarucha, L. M. K. Vandersypen, *Spins in few-electron quantum dots*, Rev. Mod. Phys. **79**, 1217 (2007).
  - [6] R. G. Knobel and A. N. Cleland, *Piezoelectric displacement sensing with a single-electron transistor*, Appl. Phys. Lett. **81**, 2258 (2002).
  - [7] R. G. Knobel and A. N. Cleland, *Nanometre-scale displacement sensing using a single electron transistor*, Nature (London) **424**, 291 (2003).
  - [8] A. D. Armour, M. P. Blencowe, and K. C. Schwab, *Entan-*

- glements and decoherence of a micromechanical resonator via coupling to a Cooper-pair box, *Phys. Rev. Lett.* **88**, 148301 (2002).
- [9] L. Y. Gorelik, A. Isacsson, M. V. Voinova, B. Kasemo, R. I. Shekhter, and M. Jonson, *Shuttle mechanism for charge transfer in coulomb blockade nanostructures*, *Phys. Rev. Lett.* **80**, 4526 (1998).
- [10] F. Pistolesi and R. Fazio, *Charge shuttle as a nanomechanical rectifier*, *Phys. Rev. Lett.* **94**, 036806 (2005).
- [11] O. Usmani, Ya. M. Blanter, and Yu. V. Nazarov, *Strong feedback and current noise in nanoelectromechanical systems*, *Phys. Rev. B* **75**, 195312 (2007).
- [12] G. A. Steele, A. K. Hüttel, B. Witkamp, M. Poot, H. B. Meerwaldt, L. P. Kouwenhoven, and H. S. J. van der Zant, *Strong coupling between single-electron tunneling and nanomechanical motion*, *Science* **325**, 1103 (2009).
- [13] B. Lassagne, Y. Tarakanov, J. Kinaret, D. Garcia-Sanchez, and A. Bachtold, *Coupling mechanics to charge transport in carbon nanotube mechanical resonators*, *Science* **325**, 1107 (2009).
- [14] G. Weick, F. Pistolesi, E. Mariani, and F. von Oppen, *Discontinuous Euler instability in nanoelectromechanical systems*, *Phys. Rev. B* **81**, 121409(R) (2010).
- [15] G. Weick, F. Von Oppen, and F. Pistolesi, *Euler buckling instability and enhanced current blockade in suspended single-electron transistors*, *Phys. Rev. B* **83**, 035420 (2011).
- [16] G. Micchi, R. Avriller, and F. Pistolesi, *Mechanical signatures of the current blockade instability in suspended carbon nanotubes*, *Phys. Rev. Lett.* **115**, 206802 (2015).
- [17] A. D. Armour, M. P. Blencowe, and Y. Zhang, *Classical dynamics of a nanomechanical resonator coupled to a single-electron transistor*, *Phys. Rev. B* **69**, 125313 (2004).
- [18] J. Koch and F. von Oppen, *Franck-Condon blockade and giant Fano factors in transport through single molecules*, *Phys. Rev. Lett.* **94**, 206804 (2005).
- [19] J. Koch, F. von Oppen, and A. V. Andreev, *Theory of the Franck-Condon blockade regime*, *Phys. Rev. B* **74**, 205438 (2006).
- [20] D. Mozyrsky, M. B. Hastings, and I. Martin, *Intermittent polaron dynamics: Born-Oppenheimer approximation out of equilibrium*, *Phys. Rev. B* **73**, 035104 (2006).
- [21] F. Pistolesi and S. Labarthe, *Current blockade in classical single-electron nanomechanical resonator*, *Phys. Rev. B* **76**, 165317 (2007).
- [22] F. Pistolesi, Ya. M. Blanter, and I. Martin, *Self-consistent theory of molecular switching*, *Phys. Rev. B* **78**, 085127 (2008).
- [23] R. Leturcq, C. Stampfer, K. Inderbitzin, L. Durrer, C. Hierold, E. Mariani, M. G. Schultz, F. von Oppen, and K. Ensslin, *Franck-Condon blockade in suspended carbon nanotube quantum dots*, *Nat. Phys.* **5**, 327 (2009).
- [24] L. Euler, in *Leonhard Euler's Elastic Curves*, translated and annotated by W. A. Oldfather, C. A. Ellis, and D. M. Brown, reprinted from *ISIS*, No. 58 XX(1), 1744 (Saint Catherine Press, Bruges).
- [25] L. D. Landau, E. M. Lifshitz, *Theory of elasticity; 2nd ed.* Pergamon, Oxford (1970).
- [26] S. Sapmaz, Ya. M. Blanter, L. Gurevich, and H. S. J. van der Zant, *Carbon nanotubes as nanoelectromechanical systems*, *Phys. Rev. B* **67**, 235414 (2003).
- [27] M. R. Falvo, G. J. Harris, R. M. Taylor II, V. Chi, F. P. Brooks Jr, S. Washburn, and R. Superfine, *Bending and buckling of carbon nanotubes under large strain*, *Nature (London)* **389**, 582 (1997).
- [28] S. M. Carr and M. N. Wybourne, *Elastic instability of nanomechanical beams*, *Appl. Phys. Lett.* **82**, 709 (2003).
- [29] S. M. Carr, W. E. Lawrence, and M. N. Wybourne, *Buckling cascade of free-standing mesoscopic beams*, *Europhys. Lett. (EPL)* **69**, 952 (2005).
- [30] D. Roodenburg, J. W. Spronck, H. S. J. van der Zant, and W. J. Venstra, *Buckling beam micromechanical memory with on-chip readout*, *Appl. Phys. Lett.* **94**, 183501 (2009).
- [31] S. L. de Bonis, C. Urgell, W. Yang, C. Samanta, A. Noury, J. Vergara-Cruz, Q. Dong, Y. Jin, and A. Bachtold, *Ultrasensitive Displacement Noise Measurement of Carbon Nanotube Mechanical Resonators*, *Nano Lett.* **18**, 5324 (2018).
- [32] A. W. Barnard, M. Zhang, G. S. Wiederhecker, M. Lipson, P. L. McEuen, *Real-time vibrations of a carbon nanotube*, *Nature* **566**, 89 (2019).
- [33] S. O. Erbil, U. Hatipoglu, C. Yanik, M. Ghavami, A. B. Ari, M. Yuksel, and M. S. Hanay, *Full electrostatic control of nanomechanical buckling*, *Phys. Rev. Lett.* **124**, 046101 (2020).
- [34] X. Wang, L. Cong, D. Zhu, Z. Yuan, X. Lin, W. Zhao, Z. Bai, W. Liang, X. Sun, G.-W. Deng, and K. Jiang, *Visualizing nonlinear resonance in nanomechanical systems via single-electron tunneling*, *Nano Research*, **14** 1156 (2021).
- [35] S. M. Carr, W. E. Lawrence, and M. N. Wybourne, *Accessibility of quantum effects in mesomechanical systems*, *Phys. Rev. B* **64**, 220101(R) (2001).
- [36] P. Werner and W. Zwerger, *Macroscopic quantum effects in nanomechanical systems*, *Europhys. Lett. (EPL)* **65**, 158 (2004).
- [37] V. Peano and M. Thorwart, *Nonlinear response of a driven vibrating nanobeam in the quantum regime*, *New J. Phys.* **8**, 21 (2006).
- [38] S. Savel'ev, X. Hu, and F. Nori, *Quantum electromechanics: qubits from buckling nanobars*, *New J. Phys.* **8**, 105 (2006).
- [39] P. Benetatos and E. M. Terentjev, *Stretching weakly bending filaments with spontaneous curvature in two dimensions*, *Phys. Rev. E* **81**, 031802 (2010).
- [40] P. Benetatos and E. M. Terentjev, *Stretching semiflexible filaments with quenched disorder*, *Phys. Rev. E* **82**, 050802(R) (2010).
- [41] P. Benetatos and E. M. Terentjev, *A constrained random-force model for weakly bending semiflexible polymers*, *Phys. Rev. E* **84**, 022801 (2011).
- [42] C.-T. Lee, and E. M. Terentjev, *Microtubule buckling in an elastic matrix with quenched disorder*, *J. Chem. Phys.* **149**, 145101 (2018).
- [43] We note that  $\alpha = \sqrt{512\tilde{\alpha}}$  where  $\tilde{\alpha}$  denotes a similar dimensionless parameter used in Ref. [15]. We note that the authors Ref. [15] take  $\tilde{\alpha} = 10^{-6}$  and  $10^{-3}$  that corresponds to  $\alpha = 0.02$  and  $0.7$ , respectively.
- [44] Y. Fan, B. Goldsmith, and P. Collins, *Identifying and counting point defects in carbon nanotubes*, *Nature Mater* **4**, 906 (2005).